Available online at www.sciencedirect.com

SciVerse ScienceDirect

Energy Procedia 37 (2013) 5570 – 5579

Energy Procedia

GHGT-11

Geochemical effects of storing CO_2 in the Basal Aquifer that underlies the Prairie Region in Canada

Stephen Talman[a]*, Ernie Perkins[a], Andrew Wigston[b], David Ryan[b], Stefan Bachu[a]

[a]*Alberta Innovates –Technology Futures, 250 Karl Clark Road NW, Edmonton, AB, T6N 1E4, Canada*
[b]*CanmetENERGY, 1 Haanel Drive, Ottawa, ON, K1A 1M1, Canada*

Abstract

In the area underlain by the Basal Aquifer in the Prairie region of Canada, there are 20 large CO_2 sources (coal-fired power plants, oil sands and heavy oil production and upgraders, refineries, chemical and petrochemical plants, fertilizer plants and cement plants) that emit more than 1 Mt CO_2/year each, for a total of 83 Mt CO_2/year, which represents 12% of Canada's annual greenhouse gas emissions. If post-combustion capture technologies are used, 75 Gt CO_2/year can be captured from these sources, with a composition (% mass) estimated to be 99.95% CO_2, 0.02% N_2/Ar/O_2, and 0.03% H_2O. The Basal Aquifer comprises Middle Cambrian sandstones that overlie the crystalline Precambrian basement in the Alberta basin and the Canadian part of the Williston basin. Shales constitute the primary caprock of the Basal Aquifer. Pressures in the aquifer generally follow a gradient of 10.8 kPa/m. Temperatures in the aquifer vary between >150ºC in the deepest part of the Alberta Basin to less than 10ºC in outcrop areas. Water salinity ranges from > 300,000 mg/L in central Alberta to < 10,000 mg/L in the southwest and in the east. The formation water in the aquifer region suitable for CO_2 storage is NaCl dominated. Generally, at in-situ conditions, these waters are saturated with $CaSO_4$ (anhydrite), with some at NaCl (halite) saturation. The mineralogy of the aquifer rocks and caprock were determined using a suite of laboratory analyses and normative calculations on core samples. The dominant mineral in the Basal Aquifer formation in regions suitable for CO_2 storage is quartz, which is generally present in the 65% to 95% range, while potassium feldspar is the next most common silicate. Pyrite is present in trace amounts in many of the samples. Calcite and illite, when present, are primarily pore-filling minerals. Calcium sulphate (anhydrite) is present in many of the samples, and, when present, is a pore-filling phase. In regard to the caprock, quartz is still a predominant mineral phase, comprising of at least one third of the rock for all samples. Potassium feldspar, illite and kaolinite are the next most common minerals. The ability of the rocks of the Basal Aquifer to react with CO_2 is limited, with potassium feldspar and complex clays providing the bulk the reactive capacity via the formation of kaolinite, or potentially a coupled reaction forming alunite and calcite in anhydrite-bearing zones. The effect of these reactions on CO_2 storage capacity, aquifer porosity and permeability is limited, allowing decoupling of flow from geochemical processes. Caprock reactivity towards CO_2 is much greater due to its more complex mineralogy, however they will not propagate far into the caprock due to its low permeability, thus allowing decoupling of flow and geochemical processes.

Selection and/or peer-review under responsibility of GHGT

Keywords: CO_2-brine-rock interactions; Basal Aquifer,Canada.

* Corresponding author. Tel.: +1-780-450-5383; fax: +1-780-450-5083.
E-mail address: Stephen.Talman@albertainnovates.ca.

Selection and/or peer-review under responsibility of GHGT
doi:10.1016/j.egypro.2013.06.478

1. Introduction

In 2009, Canada's total anthropogenic greenhouse gas (GHG) emissions were estimated to be 690 Mt of CO_2 equivalent, of which 219 Mt CO_2 eq., with a composition of 93.7% CO_2, originate from large stationary sources [1]. Most emissions from large stationary sources originate in the Prairie region of Canada (48.9 % in Alberta and 9% in Saskatchewan), where >80% of electricity is generated in coal- and gas-fired power plants and where most of the oil and gas in the country is produced and processed. An aquifer, herein referred to as the Basal Aquifer, overlies the crystalline Precambrian basement in the southern half of Alberta and Saskatchewan and southwestern corner of Manitoba, covering an area of 811,345 km^2. The CO_2 sources with individual emissions greater than 1 Mt CO_2/year in the Prairie region underlain by the Basal Aquifer (~ 83 Mt CO_2/year) account for ~40% of Canada's emissions from such sources, which is more than 10% of Canada's annual CO_2 emissions. These sources are distributed at 16 locations (Fig. 1). The volume and composition of the CO_2 stream that can be captured using a post-combustion amine-based process were estimated at each location (Table 1 in Appendix A). At locations with multiple sources, the composition of the CO_2 stream was weight-averaged. Close to 90% of the CO_2 from these sources can be captured. The water content is estimated to be 0.03%, and at most sources the concentration of non-condensable gases (N_2, Ar and O_2) is 0.01%. Condensable gases (SO_x, NO_x and H_2S) are present at three locations where the emissions are from refineries and petrochemical plants and where the captured CO_2 stream will contain these at slightly less than 10 ppm (Table 1 in Appendix A).

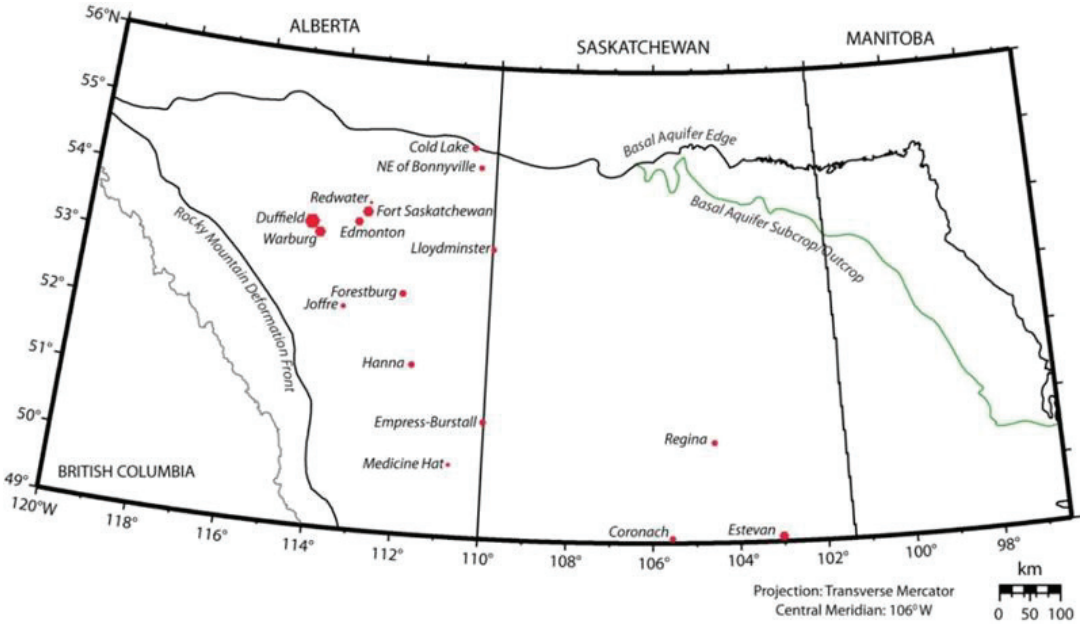

Fig. 1. Locations in the area of the Basal Aquifer in western Canada where cumulative emissions from large stationary sources are greater than 1 Mt CO_2/year. The size of the symbol is proportional with the size of CO_2 emissions (see Table 1 in Appendix A).

A 3-year bi-national effort between the United States and Canada is under way to characterize the Basal Aquifer in the northern Great Plains - Prairie region of North America and determine its CO_2 storage capacity [2] and the effects of storing CO_2 captured at large sources in the region underlain by this aquifer. This paper presents the results of studying the geochemical effects of CO_2 storage on the Canadian side of the Basal Aquifer.

2. Aquifer Mineralogy and Water Composition

In Canada, the Basal Aquifer is comprised of Middle Cambrian to Silurian sandstones and carbonates that overlie the crystalline Precambrian basement, and crops out in discharge areas in Manitoba (Fig. 1). The aquifer is overlain mostly by shales. Pressures in the aquifer follow a hydraulic gradient of 10.8 kPa/m. Temperatures in the aquifer vary between >150ºC in the deepest part of the aquifer to less than 10ºC in the outcrop area [2]. Water salinity ranges from >300,000 mg/L in central Alberta and in southeastern Saskatchewan, to <10,000 mg/L in the discharge area. Porosity varies from less than 1% in very deep regions to more than 25% in shallower regions. Using the criteria of: a) storing CO_2 at depths > 1000 m as legislated in Alberta [3], b) protecting groundwater resources with salinity <10,000 mg/L [2], and c) requiring >4% porosity [4], the area of the Basal Aquifer in Canada suitable for CO_2 storage was found to be 459,200 km^2, with a storage capacity of 86 Gt CO_2 at P_{50} confidence [2].

In the area suitable for CO_2 storage, the Basal Aquifer and its caprock consist of sandstones and shales, respectively. Samples for mineralogical analysis of Basal Aquifer rocks and caprock were selected from core taken in the region of the Basal Aquifer suitable for CO_2 storage, and high-quality water samples collected by industry and recorded with the provincial regulatory agencies were selected for determining the composition of formation water (for sample locations see Fig. 2).

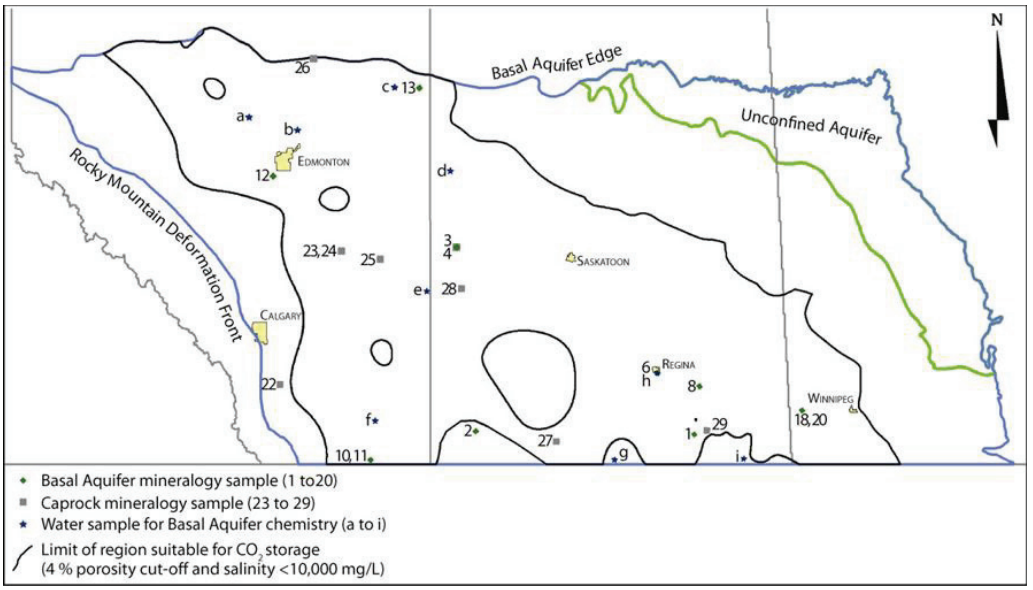

Fig. 2. Locations in the area of the Basal Aquifer in western Canada suitable for CO_2 storage where core samples were collected for mineralogical analysis and where water samples collected by industry were used for determining the composition of formation water (see Tables 2, 3 and 4 in Appendix A).

The core samples were analyzed using X-ray diffraction (XRD), SEM photomicrography and X-ray dispersive elemental analysis, and X-ray fluorescence spectroscopy (XRF). The program LPNORM [5] was used to obtain detailed composition fractions, or mineral norms, necessary for geochemical modeling. Furthermore, the aquifer minerals were constrained by requiring that they are at, or close to, equilibrium with aquifer formation water at in-situ conditions of temperature and pressure. Table 2 in Appendix A reports the calculated mineralogy of the analyzed aquifer rock samples, showing that quartz dominates (generally >80%), with K-feldspar, illite and dolomite contributing significantly to the makeup of some

samples. Commonly occurring in trace amounts are pyrite, halite and minerals generically classified as carbonates, oxides and other clays. Halite, anatase, dolomite, pyrite and hematite are identified by XRD in some samples; however, the amounts of these minerals are near the lower detections limit of this technique. The carbonates are required as a mineral host for analyzed inorganic CO_2; these incorporate excess CaO, MgO and/or Fe_2O_3. The oxides incorporate all of the analyzed TiO_2 and residual Fe_2O_3. Halite, while noted in several XRD, is likely a precipitate resulting from the evaporation of pore water recovered with the core. However, based on the salinity of recovered formation waters, it is likely absent throughout most of the aquifer. Analyzed P_2O_5. is assigned either to apatite (a calcium phosphate) or vivianite (an iron phosphate), both of which are treated as inert phases and so are not reported here. In regard to CO_2 storage, the titanium and phosphorous-bearing minerals are not expected to interact significantly. However, significant differences arise between the expected behaviour of aquifers containing iron-bearing silicates and those in which iron is present in other mineral forms. Similar mineral assemblages exist in the caprock; quartz, K-feldspar and clay minerals predominate (Table 3 in Appendix A), although, again, trace amounts of pyrite, anatase, calcite, and halite are present in many of the samples. The lower proportions of quartz and higher proportions of clays and feldspars in the caprock suggest that they have a greater reactivity to CO_2-saturated formation water than do the rocks of the Basal Aquifer itself.

Analyses of waters recovered from the Basal Aquifer at several locations close to potential CO_2 injection sites are reported in Table 4 in Appendix A (see Fig. 2 for locations). These water analyses are incomplete; reported values are restricted to Ca, Mg, Na, Cl, SO_4, alkalinity and pH. The reported Na values are commonly estimated by charge balance requirements rather than from an independent analytical determination, and as such the Na values likely include contributions from other ions, with K being of major importance. All of the waters are dominated by Na and Cl; only two water samples have more than 10% of the cationic charge (expressed as meq/L) associated with Ca and Mg, and only one sample has a combined SO_4 and HCO_3 content at more than 5% of the total anions. These waters are very saline and well outside the recommended range of the Debye-Hückel treatment of aqueous activities.

The water compositions presented in Table 4 in Appendix A were used with the geochemical modeling program PHREEQC [6] in order to calculate the saturation indices (SI) at surface conditions. The minerals were restricted to those in the system, Na, Ca, Mg, Cl, C and SO_4. All the samples are supersaturated or in equilibrium with respect to calcite. PHREEQC was also used to determine the water composition and SI's at in-situ conditions. Most samples are nearly or at equilibrium with respect to anhydrite, and oversaturated with respect to calcite. Two samples, both from near Edmonton, are close to being in equilibrium with halite, which can be expected given the proximity of Devonian salt deposits. The concentration of components not reported in the fluid analyses were estimated based on assumptions of equilibrium with common mineral phases. The K, Si, and Al concentrations were derived by dissolving kaolinite, quartz and KCl into the formation water up to the point where the water is in equilibrium with the phases kaolinite, quartz and potassium feldspar. As well, the calcite supersaturation evident at surface conditions is assumed to arise because CO_2 is lost through degassing during water sampling and sample storage. Carbon dioxide was titrated back into the solution to bring the solution into equilibrium with calcite at downhole conditions. Following these modification, the calculated saturation indices (as calculated using a reaction based on a single SiO_2 unit) of other silicate minerals in the rock tend to be relatively small, generally within about +/- 0.1. The supplemental water compositions that satisfy the equilibrium relations described above are listed in Table 5 in Appendix A. Most of the waters are essentially in equilibrium with clay minerals, generally a sodium montmorillonite, following the compositional modifications. Similarly, several samples are very nearly in equilibrium, but not oversaturated, with albite, a sodium feldspar.

3. Geochemical Modeling of Reactions between Injected CO_2 and the Basal Aquifer

The approach used here for modelling CO_2 interactions with the rocks of the Basal Aquifer is based strictly on equilibrium calculations that are fundamental to modelling all geochemical processes. Note that the kinetic data required for more complex simulations involving reaction kinetics and/or reactive transport [7], are not established for very saline waters like the ones present in the Basal Aquifer.

The geochemical model PHREEQC [6] was used in this work because it has a well-developed structure for the treatment of the thermodynamics properties of very saline brines, but the associated database is limited. An extensive, thermodynamic database, data0.ypf.r2, which was developed as part of the Yucca Mountain Project [8] was selected for this study as to be best suited for studying the interaction between the CO_2, rock and the concentrated waters of the Basal Aquifer. This database was initially developed for use with the program EQ3/6 and a modified, although largely unverified, PHREEQC-compatible version of this database [9] was used in the calculations reported here.

In-situ aqueous compositions were estimated based on analyses of recovered waters (Table 4 in Appendix A) with missing components added as noted in the previous section (Table 5 in Appendix A). These waters were brought into equilibrium with an assigned mass of minerals present in the aquifer, and a free CO_2 phase using PHREEQC [6]. The mass (in moles as required by PHREEQC) of each reactive mineral phase, relative to a one kilogram of water is approximated by

$$\text{moles mineral / kg water} = (1-\phi)/\phi_w \, \rho \, w_i / (100 \, M_i),$$

where w_i is the mineral weight percentage (see Table 2 in Appendix A), and M_i, ρ, ϕ and ϕ_w are the molar mass of the specific mineral, rock density, porosity and water-filled porosity respectively. The water-filled porosity was estimated from porosity maps which were developed over the entire aquifer and reduced, if necessary, by an estimate of the dense-CO_2 phase saturation.

Carbon dioxide is treated as an equilibrium phase as suggested in [6], with the equilibrium limited by the calculated fugacity of CO_2 at in situ conditions of initial temperatures and pressures; the pressure build-up due to CO_2 injection is neglected from these calculations (this results in a minor underestimation of CO_2 reactivity). Fugacities were calculated using AQUAtrial, a variant of the AQUAlibrium program used for acid gas phases equilibria [10]. The mass of CO_2 available for reaction was estimated for different scenarios representing the expected variations in the relative saturations of the mobile phases. During the active CO_2 injection phase, the pore space will be filled with CO_2, with water saturations reduced to residual values. Results for this CO_2/water distribution are not presented here because of space limitations. Following the cessation of injection, formation water (which is treated here as having the same composition as the original brine, i.e. not yet involved in CO_2 reactions) will displace the free CO_2 phase back to residual gas saturations. No irreducible saturations were measured on the specific cores analyzed for mineralogy, however, irreducible CO_2 saturations ranging between 0.23 and 0.51 (mean of 0.33) were obtained from seven Basal Aquifer samples [11]. In the modeling presented here a constant value of $S_{irr,CO2}$ of 0.3 was used.

The PHREEQC calculations determine the change of mass of each mineral phase required to bring the water into equilibrium with the dense CO_2 phase. Some mineral phases may completely disappear, while other phases, not initially present in the rock, may precipitate. When potential secondary phases are identified, they may be added as equilibrium phases and the PHREEQC simulation is run again. Typical results are given in Fig. 3, which shows the mineralogical changes associated with the addition of CO_2 to the Basal Aquifer system at the Estevan site. Three scenarios were modelled. The results shown with blue bars represent a case where the pore space is entirely water filled, yet there is an excess of CO_2 available. This unrealistic case yields the maximum possible CO_2 trapping. The second case (brown bars) shows results from simulations where 30% of the pore space is filled with a dense CO_2 phase; this reduces the

amount of water in the volume of rock considered and so decreases the potential for reactions to occur. The third case (green bars) is essentially the same as the second case, although with a minor amount of H_2SO_4 added to simulate the effect a small amount of SO_2 present in the CO_2 stream (0.67 wgt%, a typical concentration for CO_2 streams with SO_2 co-capture from coal-fired power plants). In each case the clay mineral, Mg-beidellite, is entirely consumed by reaction with the injected acidic gas; however, the amount of the other major silicate reactant, K-feldspar, which degrades, depends on the mass of water available. Kaolinite and quartz are the major reaction products, although a minor increase in the carbonate minerals, particularly dolomite, is also expected. Calcite, while a reaction product in the first two cases, is consumed when H_2SO_4 is included as a reactant. As expected, the CO_2 uptake via reaction was greatest for the first case (2 kg CO_2/m^3 rock), this amount was reduced by about half in the third case. This result demonstrates the impact of adding a strong acid component into an injected CO_2 stream.

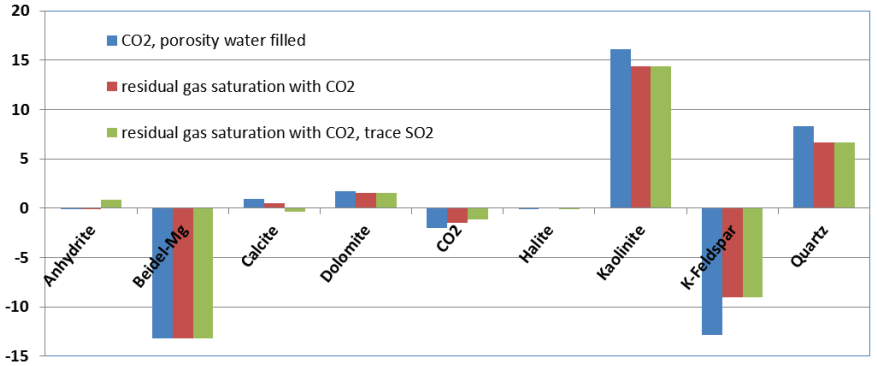

Figure 3: Calculated changes (%) in the total amount of various mineral phases following equilibration with CO_2 and H_2SO_4 for two different amounts of injected gas and water as a result of CO_2 injection into the Basal Aquifer at the Estevan site. The blue bars represent the simulation results for the hypothetical but unrealistic case in which a maximum amount of pure CO_2 is fixed.

The mineral phases dawsonite, alunite and siderite were determined to be thermodynamically stable in many of the evolved waters. Dawsonite and siderite are commonly considered reaction products in simulations of CO_2 sequestration; alunite, $KAl_3(SO_4)_2(OH)_6$, is a less-commonly noted reaction product. Its formation from a K-mica (representing a clay mineral) and anhydrite can be written as:

$$KAl_3Si_3O_{10}(OH)_2 + 2\ CaSO_4 + 2CO_2(g) + 2\ H_2O \rightarrow KAl_3(SO_4)_2(OH)_6 + 2\ CaCO_3 + 3SiO_2.$$

This reaction is driven by the activity of the CO_2 phase and results in the formation calcium carbonate. Inclusion of alunite as a secondary phase lead to a several-fold increase in the mineralogical trapping of CO_2 at some sites. However, the reaction only proceeds at relatively high CO_2 fugacity (several MPa) and the reaction may reverse itself, generating CO_2, if the CO_2 fugacity decreases below this value.

Table 1 below summarizes results of the simulations described in the preceding section for the cases based on the water/CO_2 distributions expected at residual CO_2 saturation.

Table 1: The mass of CO_2 reacted with water and minerals (fixed CO_2) at four representative sites in the area of the the Basal Aquifer suitable for CO_2 storage, compared to the mass of CO_2 that would be stored at irreducible gas saturation as free CO_2.

Site	Free CO_2 g/kg rock	Fixed CO_2 g/kg rock	% CO_2 Minerally Trapped	% CO_2 Ionically Trapped	% CO_2 in Solution
Estevan	3.8	0.95	62	2	36
Cold Lake	13.3	4.40*	63	6	30
Joffre	7.34	4.13	88	2	10
Medicine Hat	7.33	5.13	79	1	20

* Ignores potential alunite and dawsonite precipitation

Reactions between the residual CO_2 and the aquifer water and rock have the potential to fix some CO_2; (the total amount is given in the third column in Table 1). For all cases, this is less than the total CO_2 trapped at irreducible saturation (second column in Table 1). The pore space occupied by the trapped gas will decrease as a result of these reactions, but the CO_2 will disappear only as a result of the displacement of the CO_2-equilibrated water by CO_2-poor water. The low velocity of flow in the Basal Aquifer ensures that this will be a very slow process. The last three columns in Table 1 indicate the distribution of the fixed CO_2 per kg of rock mass between mineral, ionic and solubility trapping components. The values presented in Table 1 represent an upper limit. A key uncertainty is the extent to which equilibrium will be achieved between every mineral grain, the local formation water and the CO_2. Here equilibrium is assumed to be attained throughout the entire CO_2 plume, and so these results represent an upper limit.

Within the area of the CO_2 plume, CO_2-charged waters will penetrate into the caprock; farther away only aquifer water will penetrate into the caprock [12]. In both cases the composition of these waters may be approximated by the equilibrium waters determined with the previously-modelled interactions. Neither the initial aquifer nor the CO_2-charged waters are expected to be in equilibrium with caprock minerals. Their movement into the caprock is modelled here assuming local equilibrium with mass transport.

The composition of water within the caprock was estimated by equilibrating the local aquifer water with the mineralogy of the caprock (Table 3 in Appendix A). This is based on the assumption that the water/caprock interactions occurred in a relatively closed system – a small amount of water was brought into equilibrium with a large mass of caprock minerals. This initialization approach is somewhat problematic as not all mineral assemblages may exist at equilibrium; the calculation often resulted in the exhaustion of one of mineral phases in Table 3 in Appendix A (for example kaolinite, quartz, K-feldspar and a fixed composition K-clay can generally not co-exist at equilibrium). When this occurred, the target saturation indices, which define when the minerals are saturated, were adjusted to allow all minerals to co-exist. The approach can be justified as the clay minerals within the caprock are not well defined either compositionally or thermodynamically. Nevertheless, the target saturations were generally small.

Mass transport, as implemented with PHREEQC is restricted to 1-D simulation. Water equilibrated with the Basal Aquifer mineralogy was flowed through a series of cells, each representing the equilibrated caprock/water system. Aside from simple mixing of the fluids, this flow also induces reactions. Halite was present in most of the caprock samples but generally absent (and undersaturated) within the Basal Aquifer. Thus, halite dissolution was induced by flow through the caprock, as was the breakdown of iron-bearing clays. These two reactions lead to a host of other reactions. The iron released from the clay minerals remains immobile, precipitating as iron carbonate (siderite). Siderite formation removes carbonate from the solution; its source varied for different cap rock mineralogies in the caprock, but the source commonly was dolomite. Reacted waters migrating through the cells result in waves of secondary mineral precipitation within the caprock, with some simulations indicating that complex clays may form away from caprock/aquifer interface. Despite the myriad reactions induced by the migration of waters from the aquifer into the caprock far for potential injection sites, the volumes of water required to materially affect the caprock mineralogy are large. Some twenty pore volume shifts were simulated; this flow would generally strip halite from cells near the aquifer-caprock interface; however, the other primary minerals remained present in each cell.

Similar simulations undertaken to model the flow into the caprock of the Basal Aquifer water equilibrated with aquifer rocks and dense-CO_2 phase revealed similar reaction patterns, although the waters were much more aggressive. This higher reactivity resulted in the complete stripping of the more reactive primary minerals, especially the iron-bearing clays, from several cells following the twenty volume shifts. The approach used here suggests representative reactions within the caprock associated with fluid penetration into chemically-stable caprock systems both proximal and distal to potential CO_2 injection sites

4. Conclusions

Equilibrium modeling of CO_2 interactions with aquifer rocks at in-situ conditions at potential CO_2 injection sites in the Basal Aquifer in western Canada shows that, even under equilibrium conditions, the capacity of mineral-CO_2 reactions to trap CO_2 is low to moderate because of the high quartz content of the rocks and high salinity of formation waters. Additions of trace amounts of SO_2 and other acidic gas components further reduces this amount. The bulk of the injected CO_2 will remain as a free phase in the aquifer. The aquifer capacity to mineralogically trap CO_2 may be significantly enhanced in anhydrite and clay-bearing regions by the formation of calcite and the acidic potassium alumino-sulphate, alunite. This mechanism warrants further investigation. Significant changes in aquifer porosity and permeability are not expected to occur as a result of CO_2 injection. Although extensive geochemical reaction is predicted near the interface at which the CO_2-rich water comes into contact with the caprock, the reaction zone is unlikely to have sufficient thickness to exert any significant impact on the integrity of the caprock. The local impact of these reactions on CO_2 injectivity is also expected to be minor, although salt precipitation associated with drying-out of the pore space near the injection wells may pose some challenges [13], particularly at greater depths where the solubility of water in CO_2 increases as a result of higher temperatures.

Acknowledgements

The authors gratefully acknowledge financial support for this work from Natural Resources Canada, Alberta Innovates – Energy and Environment Solutions, Total E&P Canada Ltd. and SaskPower.

References

[1] Environment Canada, 2009. http://www.ec.gc.ca/ges-ghg/.

[2] Peck WD, Bachu S, Knudsen JD, .Hauck T, Chad MC, Gorecki CD, Sorensen JA, Peterson J, Melnik A. CO_2 storage resource potential of the Cambro-Ordovician saline system in the western interior of North America. *11th Int. Conf. Greenhouse Gas Control*, Kyoto, Japan, November 18-22, 2012. Energy Procedia (this volume).

[3] Province of Alberta. *Carbon Sequestration Tenure Regulation*.Alberta regulation 68/2011, Edmonton, AB, Canada. 2011.

[4] The North American Carbon Storage Atlas (NACSA), 2012. www.nacsap.org.

[5] de Caritat P, Bloch J, Hutcheon I. LPNORM: a linear programming normative analysis code. *Comp. & Geosc.* 1994, **20(3):**313-47. doi: 10.1016/0098-3004(94)90045-0**.**

[6] Parkhurst DL, Appelo CAJ. *User's guide to PHREEQC (Version 2) - A computer program for speciation, batch-reaction, one-dimensional transport, and inverse geochemical calculations.* USGS Water Resources Investigation Report. 1999, 99(4529).

[7] Xu T, Apps JA, Pruess K. Mineral sequestration of carbon dioxide in a sandstone-shale system. *Chem. Geol*., 2005, **217(3-4)**: 295–318.

[8] Sandia National Laboratories, 2007. Qualification of thermodynamic data for geochemical modeling of mineral-water interactions in dilute systems. U.S. Department of Energy, ANL-WIS-GS-000003 REV 01. U.S. Department of Energy, Office of Civilian Radioactive Waste Management. Las Vegas, Nevada, 2007.

[9] Benbow SJ, Metcalfe R, Wilson J. *Pitzer database for use in thermodynamic modelling*. Quintessa QRS-3021A-TM. 2008.

[10] Carroll JJ. The water content of acid gas and sour gas from 100° to 220°F and pressures to 10,000 psia. 2002. 81st Annual Gas Processors Association Convention , March 11-13, 2002, Dallas, Texas, USA.

[11] Bachu S. Drainage and imbibition CO_2/brine relative permeability curves at in situ conditions for sandstone formations in western Canada. *11th Int. Conf. Greenhouse Gas Control Technologies*, Kyoto, Japan, November 18-22, 2012, Energy Procedia (this volume).

[12] Birkholzer JT, Zhou Q. Basin-scale hydrogeologic impacts of CO_2 storage: Capacity and regulatory implications. *Int. J. Greenhouse Gas Control*. 2009, **3(6)**:745-56.

[13] Pruess K. Müller N. Formation dry-out from CO_2 injection into saline aquifers: 1. Effects of solids precipitation and their mitigation. *Water Resour. Res*. 2009, **45,** W03402

Appendix A. Data Tables.

Table 1: Estimated volume and composition of the CO_2 stream captured using post-combustion amine-based processes for the large CO_2 sources at the locations in the area of the Basal Aquifer in the Prairie region of Canada where more than 1 Mt CO_2/year are emitted from large stationary sources.

Location	2009 CO_2 Emissions (kt/yr)	Captured CO_2 (kt/yr)	Stream Composition					
			Mass %			Concentration (ppm)		
			CO_2	N_2/Ar/O_2	H_2O	SO_x	NO_x	H_2S
Bonnyville	4,882	4,394	99.97	0.01	0.03	0	0	0
Cold Lake	4,333	3,900	99.97	0.01	0.03	0	0	0
Coronach	4,215	3,793	99.97	0.01	0.03	0	0	0
Duffield	16,110	14,499	99.97	0.01	0.03	0	0	0
Edmonton	5,047	4,542	99.84	0.13	0.03	1.1	1.5	3.4
Empress	4,106	3,608	99.97	0.01	0.03	0	0	0
Estevan	9,526	8,573	99.97	0.01	0.03	0	0	0
Forestburg	5,148	4,633	99.97	0.01	0.03	0	0	0
Ft. Sask.	6,070	5,409	99.93	0.04	0.03	0.3	0.4	0.9
Hanna	4,863	4,377	99.97	0.01	0.03	0	0	0
Joffre	2,712	2,467	99.97	0.01	0.03	0	0	0
Lloydminster	2,423	2,152	99.97	0.01	0.03	0	0	0
Medicine Hat	1,718	1,574	99.97	0.01	0.03	0	0	0
Redwater	1,003	919	99.97	0.01	0.03	0	0	0
Regina	1,708	1,537	99.77	0.21	0.03	1.7	2.4	5.5
Warburg	9,490	8,541	99.97	0.01	0.03	0	0	0
Total	**83,354**	**74,918**	**99.95**	**0.02**	**0.03**			

Table 2: Mineralogical composition of aquifer rock samples taken from core in wells that penetrate the Basal Aquifer in the region suitable for CO_2 storage in Canada as determined using LPNORM. The "Ca-Sulphate" entries represents either anhydrite or gypsum, while the "Oxides" row represents the oxides and hydroxides of iron and titanium. The "Other clays" entries represent clays more complex than kaolinite and illite; these are required as mineral hosts for Mg in some samples. The carbonate row generally represents calcite and/or siderite. The location of the samples is shown in Fig. 2.

Mineral	Aquifer Rock Sample											
	1	2	3	4	6	8	10	11	12	13	18	20
Quartz	97.2	75.5	91.3	29.5	98.2	90.1	97.7	98.0	92.7	82.1	85.1	75.2
K-Feldspar	0.9	15.3	2.7	31.9	0.7		1.6		1.8	7.6	0.8	
Dolomite		1.0		25.1	0.6							
Illite		4.9		10.9		7.8			2.3			
Ca-Sulphate										7.8	5.9	15.1
Pyrite			0.2			0.7	0.1	0.6			4.8	5.7
Other Clays	1.3		1.5		0.5			0.7	2.3	1.7		
Oxides		3.1		1.9			0.3	0.3	0.6			0.1
Analcime											2.0	3.9
Carbonates	0.4	0.2	0.5			0.9	0.3	0.4		0.9	0.9	
Kaolinite			3.3									
Halite	0.2		0.5	0.7		0.4			0.3		0.4	0.1

Table 3: The major mineralogical composition of the caprock samples taken from core in wells that penetrate the Basal Aquifer in the region suitable for CO_2 storage in Canada. The notes regarding mineral groupings in Table 2 above apply here as well. For location of the samples see Fig. 2.

Mineral	Caprock Sample							
	22	23	24	25	26	27	28	29
Quartz	36.9	21.0	8.5	30.3	19.2	16.9	11.9	39.6
K-feldspar	10.0	27.0	19.9	27.0	11.2	20.0	30.0	20.1
Kaolinite	10.9	5.9	33.4		2.0	14.4	12.8	15.1
Other clays	34.6	23.2	24.0	23.6	26.0	41.2	21.6	15.3
Dolomite		15.2	3.0		29.8	1.0	17.9	0.8
Calcite				13.6	1.1	1.8		
Carbonates	2.1							
Halite	0.4	0.7			1.6		0.8	
Anhydrite					5.7			
Oxides	0.9	1.0	1.0	1.5	0.3	0.8		
Pyrite	0.9	1.0	2.9			0.3		5.8

Table 4: Analyses of water taken in vicinity of prospective CO_2 injection sites in the Basal Aquifer in western Canada. A temperature of 23ºC was assumed for the pH measurement. For location of the samples see Fig. 2.

Location Fig. 1	ID Fig. 2	T (ºC)	P (MPa)	Density (kg/m^3)	pH	Cations (g/L)			Anions (mg/L)		
						Na	Ca	Mg	Cl (g/L)	C[1]	S[2]
Cold Lake	c	50	12.2	1162.0	7.5	94.5	1.79	0.85	147.0	40	1,900
Coronach	g	80	28.7	1093.5[3]	6.4	49.3	1.95	1.08	80.5	84	894
Edmonton	b	60	21.1	1210.0	5.7	114.9	3.14	1.97	187.3	106	384
Estevan	i	100	32.5	1253.0	5.4	97.5	23.62	2.07	198.0	21	90
Joffre	e	70	26.0	1214.2	6.4	115.8	4.96	0.96	189.7	81.6	366
Lloydminster	d	50	14.9	1164.0	6.4	90.7	2.12	0.87	143.7	43	1,027
Medicine Hat	f	70	20.2	1036.0	8.1	13.4	0.50	0.14	20.8	385	47
Regina	h	60	22.1	1082.0	7.9	46.4	1.40	0.37	71.9	62	1,384
Warburg	a	80	28.7	1213.0	6.1	107.2	15.33	2.62	199.8	10	110

[1] Reported alkalinity converted to bicarbonate and reported as C; [2] Reported SO_4^{-2} is reported here as S; and [3] estimated from TDS.

Table 5: Calculated composition (in moles/kg H_2O) of formation water samples of Table 4 above equilibrated with calcite, K-feldspar, quartz and kaolinite. For location of the samples see Fig. 2.

Location Fig. 1	ID Fig. 2	Al	K (moles/kg)	Si (moles/kg)	C (moles/kg)	Fugacity CO_2 (MPa)	pH @T
Cold Lake	c	5.1×10^{-10}	1.72×10^{-2}	2.10×10^{-4}	4.67×10^{-3}	6.63	5.99
Coronach	g	7.8×10^{-11}	3.16×10^{-2}	5.27×10^{-4}	1.20×10^{-2}	12.91	5.63
Edmonton	b	5.2×10^{-9}	5.75×10^{-2}	2.49×10^{-4}	1.16×10^{-2}	9.13	5.34
Estevan	i	1.5×10^{-9}	1.00×10^{-1}	6.26×10^{-4}	3.31×10^{-3}	16.23	4.87
Joffre	e	2.7×10^{-8}	9.44×10^{-2}	1.76×10^{-4}	1.07×10^{-2}	11.17	5.18
Lloydminster	d	5.9×10^{-10}	1.95×10^{-2}	2.10×10^{-4}	4.45×10^{-3}	7.13	5.94
Medicine Hat	f	1.1×10^{-10}	4.91×10^{-2}	5.06×10^{-4}	1.26×10^{-1}	9.81	5.50
Regina	h	7.8×10^{-11}	1.78×10^{-2}	3.41×10^{-4}	8.67×10^{-3}	9.33	6.00
Warburg	a	3.1×10^{-10}	2.56×10^{-2}	3.94×10^{-4}	1.00×10^{-3}	12.91	5.54